

## Evaluation of Anticorrosive Effect of Niobium Carbide Coating Applied on Carbon Steel

Luisa Novoa<sup>b</sup>, Luis E. Cortes<sup>a</sup>, Eliana Gonzalez<sup>b</sup>, Arnaldo Jimenez<sup>a</sup>, Luis G. Cortes<sup>a</sup>, Mario Ojeda<sup>a</sup>, Aida L. Barbosa<sup>\*a</sup>

<sup>a</sup> Laboratory of Research of Catalysis and New materials (LICATUC), Science Faculty, Chemistry Program, University of Cartagena, Campus of Zaragocilla, Kra 50 N° 30-40, Cartagena, Colombia

<sup>b</sup> Dept of Civil Engineering, Civil Engineering program, University of Cartagena, Campus of Piedra de Bolivar, Av. El Consulado Calle 30. No. 48 - 152, Cartagena, Colombia  
[abarbosal@unicartagena.edu.co](mailto:abarbosal@unicartagena.edu.co)

South America and particularly Colombia, has niobium and tantalum deposits, which can be used as a carbon steel protective agent. A preliminary step is the raw material characterization. Fresh and calcinated samples of niobium mineral in ores and sand were analyzed through optic microscopy, laser-Raman spectroscopy, DRX and textural aspects. The main components of the ore and alluvial sand were Ferrotapiolite and ferrocolumbite with chemical formula  $(\text{Fe,Mn})\cdot(\text{Ta,Nb})_2\text{O}_6$  and associated oxides like  $\text{Fe}_2\text{O}_3$ ,  $\text{SiO}_2$ . In the shape of Tectosilicates, Mn-Tantalite, Nb=O terminal and polyatomic octahedral structures of  $\text{NbO}_6$ , highly distorted, susceptible to form carbides. Ferrocolumbite synthetic (FeNb50) was used as precursor of NbC coating for the surfaces protection of AISI 1020 steel samples having dimensions of 3/8 inch diameter and 1/2 inch length. The film was obtained by thermoreactive deposition at atmospheric pressure. The anticorrosive effectiveness of 9 thermic treatments was tested through accelerated corrosion tests and verified by Raman spectroscopy. The formation of a hard coating of NbC was identified using Energy Dispersive X-ray Spectroscopy (EDS), in a very small range between 950°C for 2.5h and 1000°C for 1.5h, in presence of  $\text{Fe}_3\text{C}$ , corresponding with the lowest oxidation percentages. SEM microscopy shows a rough and uneven surface. The intervals of thickness of 4  $\mu\text{m}$  to 137.2  $\mu\text{m}$ , measured with a MCT-300. Bonds between Nb-C and Fe-C,  $\text{Nb}_2\text{O}_5$  and  $\text{NbO}_6$  species were appreciated with the Laser-Raman spectroscopy after the oxidation process.

### 1. Introduction

Corrosion can be defined as a chemical or electrochemical reaction between a material, generally a metal, and its environment, which leads to the decay of the material and its properties. This process depends fundamentally on the relative humidity, air composition and the contaminants present on it, such as sodium and chloride. Beyond a few hundred meters away from the sea line, salinity and corrosion speed tend to decrease ostensibly. Recent studies performed with the goal of improving anticorrosive properties of steel have been focused on hard coatings, their production and characterization. Carbide films of transition metals, such as vanadium and niobium, have gained research relevance. These carbides present an unusual combination of physicochemical properties, such as high fusion temperatures, high hardness and corrosion resistance (Ramirez et al., 2013). Niobium, also known as columbium, is found as part of the mineral Columbite (or niobite)  $[(\text{Fe,Mn})\text{Nb}_2\text{O}_6]$ , its main uses are in form of ferroniobium as blending for steels and as Niobium carbide in steel tools for high speed machining. One technique used for the synthesis of coatings for carbon steel is known as Thermo-Reactive Deposition/Diffusion (TRD), the hard layers of metallic carbide are formed by reaction among the carbon atoms, which spread from the steel, used as substrate, and the carbide atoms forming element that is intended to be implanted, it can be vanadium, niobium or chrome. Carbide forming elements (CFE) are added as powder ferroalloy into a molten bath of Sodium Tetraborate Pentahydrate (borax). The free Carbon present in steel combines with the CFE in order to produce a superficial hard layer. The layer grows as the Carbon from the substrate, reaches the surface to

react with the atoms of the CFE to finally obtain, depending on the CFE, layers composed of Niobium carbides (NbC), Vanadium carbides (VC), among others, on the steel surface. In Colombia is possible to find minerals of Niobium and Tantalum, known as Coltan, these are strategic for the development of the country. Therefore the main goal of this research was to determine the richness of ferroniobium in ores and alluvial samples of the Colombian mineral, which may become a cost-effective alternative to produce an engineering material as NbC. In this study an accelerated corrosion assay and Raman spectroscopy were used to test its anticorrosive effectiveness by applying it on structural steel AISI 1020. Results showed that precursor salt ferroniobium 50 yielded hard coatings, formed it's in thermo-reactive diffusion process, in the presence of iron carbide, that benefit the anticorrosive effect in a small intervals under very specific conditions.

## Experimental

Raw niobium samples from the Guainia-Colombia region (ore and sand), went through a physicochemical analysis. Firstly, the raw ore mineral samples were macerated in a steel mortar, until a 100 mesh particle size and homogeneity were reached. The texture was analyzed by optic microscopy in a C-LEDS model NIKON microscope coupled to an AmScope camera, and the possible transformations of the crystalline structure were to be observed through LASER-RAMAN spectroscopy in a BaySPEc 1064nm equipment.

### 2.1 Steel sample preparation and Niobium carbide coating application

Preparation, cleaning and evaluation of carbon steel samples used for corrosion tests were done using the ASTM G1-90 Standard Guide. For the elaboration of the samples, an AISI 1020 steel bar with diameter (3/8) inch was used, divided in 40 sections of (1/2) inch of. The pieces of steel were subsequently polished with an electric bench grinder and then cleaned with a weak mixture of citric and acetic acid in order to remove greases and oils from the surface. The acid was then removed with ammoniac aspersions, and finally dried with towels. Niobium Carbide (NbC) coatings were made considering some variables for the film depositions, like the time and temperature of the thermic treatment. The test pieces were taken to the furnace with 81% borax, 16% Ferro-alloy (Ferro niobium) and 3% of aluminum in the mixture, using a graphite cresol, Ramirez (2013). Test samples were elaborated following different treatments, varying the temperature and exposure time on the furnace, as shown on Table 1.

Table 1: Total treatments performed in coating synthesis.

Treatment	Time(hours)	Temperature (°c)	N° test pieces
1		900	4
2	1,5	950	4
3		1000	4
4		900	4
5	2,5	950	4
6		1000	4
7		900	4
8	3,5	950	4
9		1000	4

Then samples were exposed to the simulated saline environment into a chamber of saline fog. The coating formation and its surface morphology were examined through Scanning Electron Microscopy (SEM), its thickness was measured with a Minipa MCT-300.

### 2.2 Evaluation of degree of rusting on NbC coating in saline chamber exposure tests

Norm ASTM B 117 was used for the accelerated corrosion tests employing saline fog in a Q-FOG CCT-600 to 640 Liters chamber. For the entry to the chamber protocol, were take 4 groups (A (10h), B (30h), C(50h), D(100h) ), with 10 samples each one, which were coming of the nine thermic treatments and one control sample, Each sample group entered to the chamber at different times, until the exposure temperature established for the study table 2. The identification of the phases of the oxides, associated with the corrosive processes, was done by Laser-Raman. For the calculation of the percentage of oxidation in the surface of the test pieces was used the ASTM D 610 standard test recommendations.

## 3. Results

### 3.1 Analysis of optic microscopy and Raman spectrometry

The sand sample showed the presence of magnetite, zircon, Ilmenite, quartz crystals and feldspars (Cramer,et al.,2011), The minerals from the columbite group, composed of 4 members: columbite-(Fe),

columbite-(Mn), tantalite-(Fe) and tantalite-(Mn), were observed in each phase of the ore samples, (Chakhmouradian, et al., 2015). Raman frequencies were strongly dependent on the niobium oxide structures, indicating a higher richness in the ore sample than in the sand sample (Figure 2a). The bands present at  $846\text{ cm}^{-1}$  up to  $900\text{ cm}^{-1}$  are related with octahedral  $\text{Nb}_2\text{O}_5$ , with symmetric stretching between  $440\text{ cm}^{-1}$  and  $800\text{ cm}^{-1}$  (Jenhg and Wachs, 1990). The wide band in  $680\text{ cm}^{-1}$  was associated to  $\text{NbO}_6$  and  $\text{NbO}_7$  units, present in  $\text{Nb}_2\text{O}_5$ , the band around  $900\text{ cm}^{-1}$  was related to the  $\text{Nb}=\text{O}$  terminal bonds. For the lightly distorted octahedral  $\text{NbO}_6$  structures ( $\text{KNbO}_3$ ,  $\text{NaNbO}_3$ ,  $\text{LiNbO}_3$ ) present in the sand samples, appear in  $500\text{ cm}^{-1}$  to  $700\text{ cm}^{-1}$ . For the highly distorted octahedral structures  $\text{K}_8\text{Nb}_6\text{O}_{19}$ ,  $\text{AlNbO}_4$ ,  $\text{Nb}(\text{HC}_2\text{O}_4)$ , the main Raman frequencies move from the  $500\text{ cm}^{-1}$  to  $700\text{ cm}^{-1}$  range to the region around  $850\text{ cm}^{-1}$  to  $1000\text{ cm}^{-1}$  in the ore sample.

The XRD diffraction pattern of the sand samples and raw ore at room temperature showed that these minerals are highly crystalline. The ore sample shows peaks at  $2\theta = 18.4^\circ$  and  $31.2^\circ$  which could correspond to  $\text{Fe-Ta}_2\text{O}_5$   $\text{KTiNbO}_5$  respectively. Presence of  $\text{Fe-Nb}_2\text{O}_5$  at  $2\theta = 30.6^\circ$  and  $27.8^\circ$ ; and tantalum oxides at  $2\theta = 24.1^\circ$  and  $23.4^\circ$ , Gubernat (2013). The peaks at approximately  $2\theta = 15.4^\circ$  and  $36.5^\circ$  are attributed to mineralization of zeolites such as cristobalite and Yugawaralite respectively. For the sand show typical signals at crystal niobium and tantalum phases associated to Fe and Mn, which correspond to  $2\theta = 27.6^\circ$  y  $55.8^\circ$ . The possible main components of the ore and alluvial sand samples were ferrotapiolite and ferrocolumbite of chemical formula  $(\text{Fe,Mn})\cdot(\text{Ta,Nb})_2\text{O}_6$ , being the last one the material with potential for the development of metallic Iron-Niobium Carbides (Kabangu and Crouse,2012 ; Rodriguez, et al., 2007).

### 3.2 Coating chemical composition and morphology analysis

The Niobium Carbide coatings were analyzed through Scanning Electron Microscopy (SEM) combined with Energy-Dispersive Spectroscopy (EDS). The analysis was performed on the transversal section of the substrate-coating system and on a point of the formed layer, yielding the results from Figure 3 and Table 2. Temperature dependence in the metallic carbide coatings was evidenced in the formation of the layers and their uniformity. Samples TA900-1, TA900-2 did not allow to differentiate the structure of the layers and an amorphous material with a very heterogeneous distribution of components was obtained.

Table 2: Percentual chemical composition of coating by EDS

T t.	% wt elements			
	C	Nb	Fe	O
1	4.2	0	42.7	37.8
2	4.1	2.5	72.1	11.6
3	2.1	17	56.3	14.1
4	3.8	0	1.7	41.1
5	15.9	0.2	15.2	39.4
6	14.6	49.2	26.8	7.2
7	6.1	74.9	9.9	9.1
8	10.3	77.5	3.8	8.5
9	44.4	3	16.2	21.9

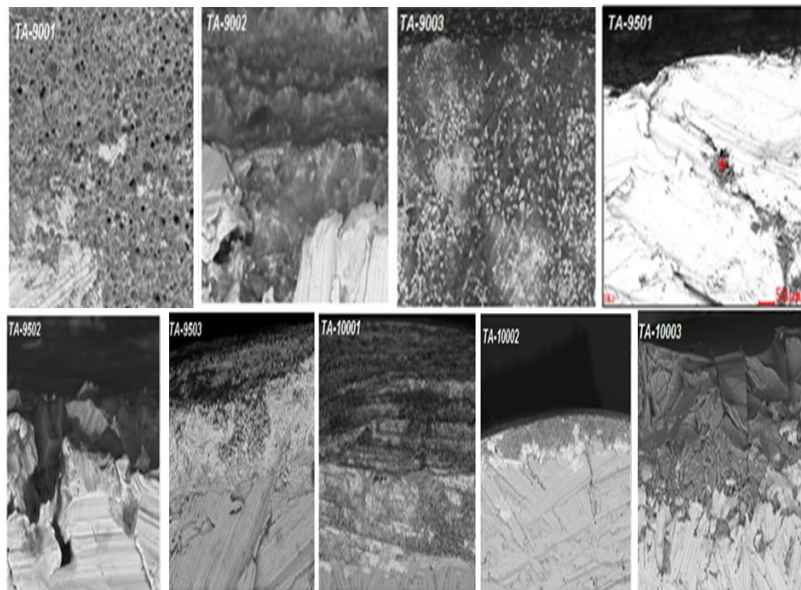


Figure 1: Description of the morphology and texture of the test pieces after Thermo-Reactive treatment.

Dispersed particles of  $\text{FeC}$  were distinguished, which could be related to the amount of synthetic Ferroniobium employed, it was very important for the formation of Niobium Carbide at higher temperatures. In our case just the coatings obtained from the specimens TA1000-2, TA900-3 and TA950-3, presented regular and compact layers over the substrate surface. It can be seen that the composition of the Ferroalloy was responsible of the porosity and inclusions found in the substrate. Increasing the temperature, samples TA950-2 and TA1000-1 showed more grey and light grey color zones with shine and clearer particles distributed on the surface, (Li, et al., 2014) show that this areas and clearer particles are conformed by Niobium Carbide. This agrees with the

resulting percentual composition by EDS (Table 2), in which the greater areas are richer in Niobium, in comparison with the small particles, in which Carbon and Niobium are present in equal percentages. Finally increasing the temperature and exposure time for specimen TA1000-3, differentiated layers can be observed; one very fractured, more dense and dark. It can be noted that only two samples were propitious for the formation of the Niobium Carbide as coating of the AISI 1020 steel, TA1000-2 reached a 14.63% of C and 40.21% Nb, and TA 950-3 reached 10.29% of C and 77.46% Nb. In Figures 4a and 4b, ratio curves of the increase of coating thickness in relation to temperature and treatment time are shown, respectively. Generally is appreciated that treatment with: exposure times of 1.5h and temperature of 900°C gave lower thickness changes. At 950°C and 2.5h was hard to control the variability of the obtained thickness. Temperatures of 1000°C and 3.5h times lead to higher thicknesses in a wide range of measures. Nevertheless, it should be noted that the increase in the coating thickness was not closely related to the amount of Niobium Carbide (Table 2), (Rodriguez, et al., 2007; Guerrero, 2013).

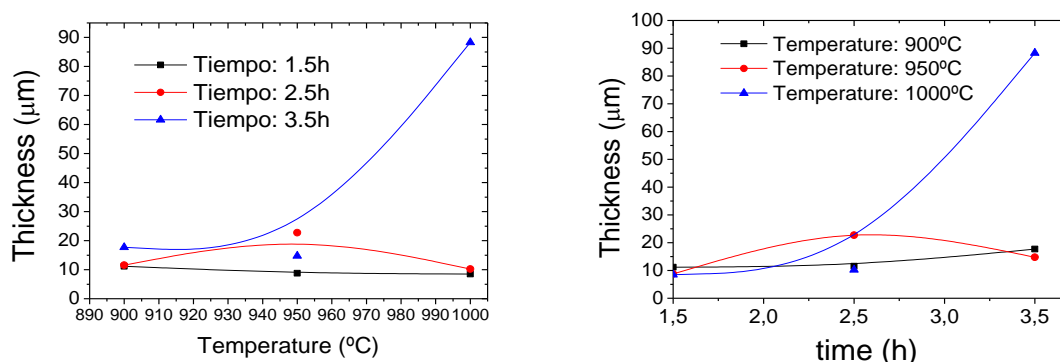


Figure 4: Coating thickness increment in regard to a - Temperature b - Time.

### 3.3 Behavior of the metallic coatings of Niobium Carbide grown over the AISI 1020 substrate.

For studying the performance of the synthesized Niobium Carbide coatings, test pieces from the 2 and 9 treatments were chosen, in the conditions pointed in Table 3. The most promising results were obtained in treatments 6, 7 and 8, that, as stated previously, possess a higher content of metallic NbC Carbide formed over the AISI 1020 substrate.

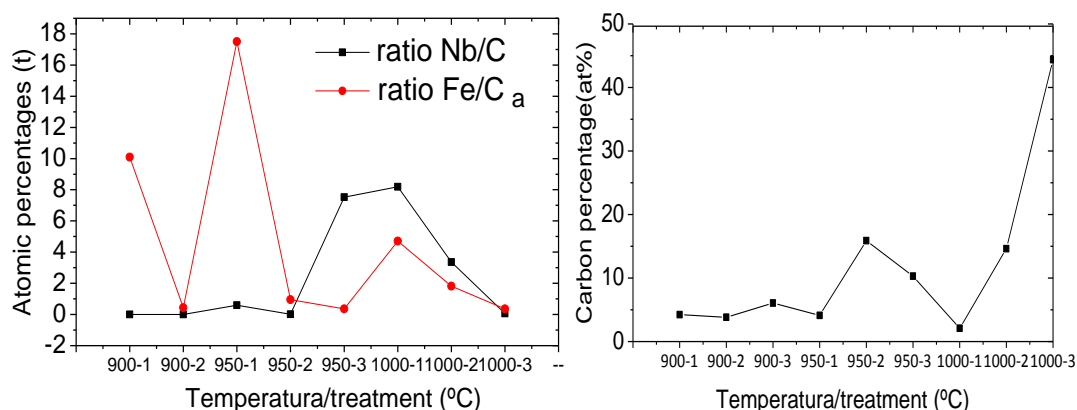


Figure 5: Relations of the Nb/C, Fe/C ratios. b) Percentage of Carbon vs. the treatment temperature.

The dependency of the atomic percentages of Niobium and Iron, for the samples grown over the AISI 1020 substrate, Figure 5, showed that near 950°C, 3.5h begins the formation of Niobium Carbides possibly of the interstitial type. Even though it was observed that increasing the temperature facilitated the formation of Nb-C bonds, Carbon percentage and thickness of the film were increased as well, (Figure 4), it was inferred that the range in which the NbC was produced, was to small, between 950°C with higher exposure times in the furnace and 1000°C with short times. At higher times, the niobium stopped taking in Carbon and expeled it, figure 5b. The increase of Carbon at higher temperatures 1000°C and 2.5h exposure times could be impeding the carbide phase formation (Li, et al., 2014). Besides a drastic change was observed in the carbon

percentage curve above 1000°C degrees, this could be related to with the preference to form pyrolytic coke, this carbon specie is observed, if the metal carbide was formed before. (Zhang, et al, 2016). The Iron Carbide had a drastic changing behavior (Figure 5a) because it have structural variants. At temperatures below 150°C Iron Carbide nuclei with compact hexagonal structure are formed, type Fe<sub>2.5</sub>C, up to 350°C the structure was ordered forming sheet of Carbide at high temperatures name cementite, Fe<sub>3</sub>C (Zheng, et al., 2012), It was, (figure 5a) beneficial for the production of an alloyed material, that presents resistance to corrosion.

Table 3: Percentage of area oxidation on the AISI 1020, steel test piece vs. hours of exposure to the saline fog chamber.

		% Oxidation Area vs. hours in chamber								
Treatment	Codes	10h (A*)	24h (B y D*)	30h (B*)	48h (D*)	50h (C*)	72h (D*)	100h (D*)	Mean (%)	
2	T(*)900-2	10	41.5	100	100	100	100	100	78.8	
3	T(*)900-3	3	33.0	100	100	100	100	100	76.6	
6	T(*)950-3	0	6.5	10	50	100	100	100	52.4	
7	T(*)1000-1	3	13.0	50	50	100	50	100	52.3	
8	T(*)1000-2	0	13.0	50	33	100	100	100	56.6	
9	T(*)1000-3	0	25.5	33	100	100	100	100	65.5	
Blank	B(*)	10	41.5	10	100	100	100	100	65.9	

\*Code Letter indicates the group of the test piece according to the entry to the chamber and the total exposure hours

### 3.4 Identification of oxides present in the coatings after exposure to the Saline fog chamber.

For the identification of the oxides phases associated with the corrosion processes in the AISI 1020 steel test pieces, representative samples of each of the treatments were selected after 100 hours of exposure in the Saline fog chamber.

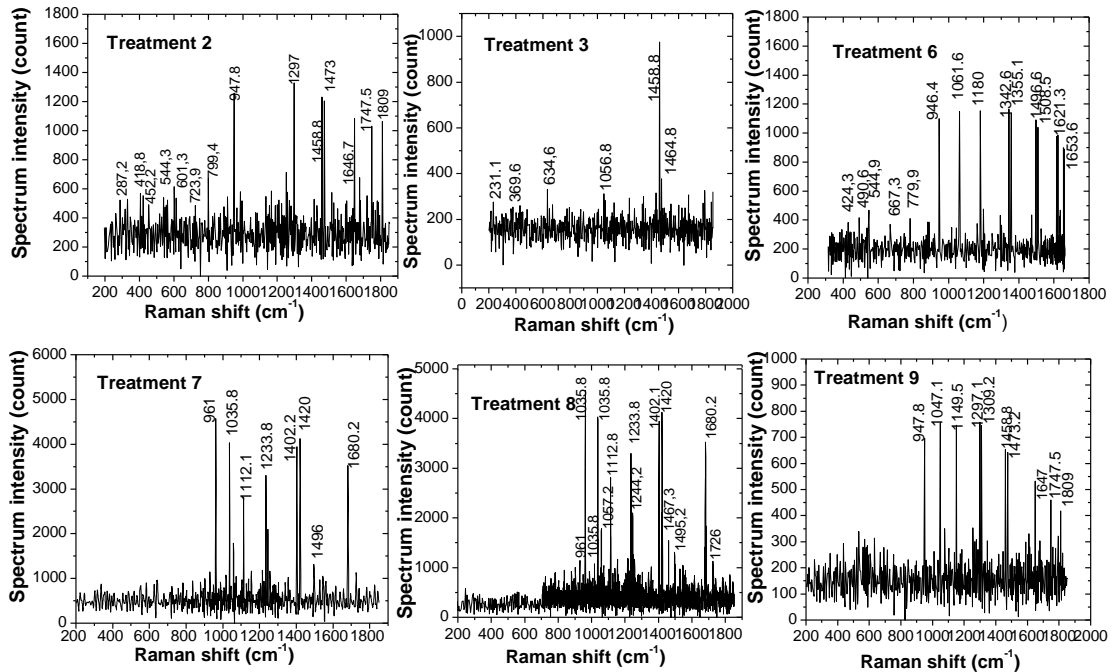


Figure 4: Raman spectra of the different treatments after 50 hours of exposure to the Saline fog chamber

Raman bands between 950 cm<sup>-1</sup> and 1700 cm<sup>-1</sup>, could be related to the type of carbon structures present in metallic carbides. In general it was not possible to appreciate the phases related to the Iron corrosion as hematite. On the other hand, is highlighted that band at 1580 cm<sup>-1</sup>, called “graphitic peak”, which indicated

graphitization, did not appear in any of the cases, this result was to be expected because Niobium, inhibits this phenomenon (Anoshkin, et al., 2017). After 50h of exposure in oxidant conditions, octahedral NbO<sub>6</sub> structures and terminal type Nb=O bonds were appreciated, instead of NbC. The treatments 7 to 9, lead to fivefold coordinated NbO<sub>5</sub>, in 930cm<sup>-1</sup> to 950cm<sup>-1</sup>, whilst treatments 2, 3 and 6 favored the sixfold coordinated NbO<sub>6</sub> species, with band in the 630cm<sup>-1</sup> to 650cm<sup>-1</sup> interval (Jenhg & Wachs, 1991). In the formation of the metallic Carbides and in its oxidation processes, the amorphous transformation of Carbon, evidenced in the bands at 1340cm<sup>-1</sup> was important, additionally up 1000°C may generate carbon polymerization to produce the Carbide, with an enrichment of the Raman signals between 1400cm<sup>-1</sup> and 1600cm<sup>-1</sup> (Cruz, et al., 2017).

## 2. Conclusion

Coatings based on Niobium Carbide were prepared with the Thermo-Reactive Deposition/Diffusion method, the quality of layers of NbC depended on the adjustment of the reaction parameters (such as composition of the bath of molten salts, reaction temperature, reaction time, molar ratio of metals and Carbon percentage). An increase in the thickness of the coatings was appreciated with an increase in the reaction temperature and time. The Raman signals between 1400cm<sup>-1</sup> and 1600cm<sup>-1</sup> after oxidation process in all the treatments were associated with the thermal transformation in the Carbon constituent of the Carbides.

## Acknowledgments

The authors acknowledge the financial support of the administrative department of science and technology Colciencias by the project, 004-2016 Geosciences Program. Arnaldo Jimenez is grateful to Colciencias, for Master grant by project 004-2016. To Cartagena University for sustainable project 2015-2016.

## References

- Anoshkin, I., Nefedova, I., Lioubtchenko, D., Nefedov, I., & Räsänen, A. (2017). Single walled carbon nanotube quantification method employing the Raman signal intensity. *Carbon*, 547-552.
- Chakhmouradian, A., Reguira, E., Kressallb, R., Crozier, J., Pisiakd, L., Sidhu, R., . . . Sidhua, R. (2015). Carbonatite-hosted Niobium deposit aley, northern British Columbia(Canada): Mineralogy, Geochemistry and petrogenesis. *Ore Geology Reviews*, 642-666.
- Cramer, T., Amaya, Z., Franco, J., Bonilla, A., & Poveda, A. (2011). Caracterizacion de depositos aluviales con manifestaciones de Tantalio y niobio ("Coltan") en las comunidades indigenas de Matraca y Caranacoa, departamento del Guainia. Bogotá: Ingeominas, Universidad Nacional de Colombia.
- Gubernat, A. (2013). Pressureless sintering of single-phase tantalum and Niobium carbide. *Journal of European Ceramic Society*, 2391-2398.
- Guerrero, F. A. (2013). Resistance to corrosion in coatings of Vanadium Carbide and Niobium Carbide deposited with the TRD technique. National University of Colombia.
- Jenhg, J., & Wachs, I. (1991). Structural chemistry and Raman spectra of Niobium oxides. *Chemistry of materials*, 100-107.
- Kabangu, J., & Crouse, P. (2012). Separation of niobium and tantalum from Mozambican tantalite by ammonium bifluoride digestion and octanol solvent extraction. *Hydrometallurgy*, 151-155.
- Li, Q., Lei, Y., & Fu, H. (2014). Laser cladding in-situ NbC particle reinforced Fe-based composite coatings with rare earth oxide addition. *Surface & Coatings Technology*, 102-107.
- Mendez, J., Bosh, P., & Lara, V. (1996). FTIR spectroscopy and X-Ray diffraction characterization of Nb doped Sol-Gel silica. *Journal of Sol-Gel Science and Technology*, 257-262.
- Ramirez, M. (2013). Evaluation of the resistance to wear of Niobium carbide (NbC), Vanadium Carbide (VC) and Ternary Carbide of Niobium and Vanadium (NbVC) produced by the thermal-reactive diffusion technique (trd). Bogota, Colombia.
- Rodriguez, M., Ojala, N., Katsich, C., Totolin, V., Tomastik, C., & Hradil, K. (2016). The role of niobium in improving toughness and corrosion resistance of high speed steel laser hardfacings. *Materials & Design*, 509-520.
- Zhang, L., Zhang, T.D., Gao, R., Tang, D.Y., Tang, J.Y., Zhan, Z.L. (2016). Preparation and characterization of mesoporous carbon materials of chinese medicine residue with high specific surface areas, *Chemical Engineering Transactions*, 55, 79-84
- Zheng, B., Huang, Z., Xing, J., Xiao, Y., Fan, X., & Wang, Y. (2012). Effects of Chromium Addition on Preparation and Properties of Bulk Cementite. *Surface and Coatings Technology*, 169-179.